Parametric dynamic interaction assessment between bells and supporting slender masonry tower

Parametric dynamic interaction assessment between bells and supporting slender masonry tower

David Bru

Department of Civil Engineering. University of Alicante, Alicante 03690, Spain

Email: david.bru@ua.es

https://orcid.org/0000-0001-7567-1560

Salvador Ivorra

Department of Civil Engineering. University of Alicante, Alicante 03690, Spain

Email: sivorra@ua.es

http://orcid.org/0000-0002-8647-8173

Michele Betti

Department of Civil and Environmental Engineering.

University of Florence, Florence I-50139, Italy

Email: mbetti@dicea.unifi.it;

http://orcid.org/0000-0002-8389-3355

Jose M. Adam

ICITECH, Universitat Politècnica de València, Camino de Vera s/n, Valencia, Spain

Email: joadmar@upv.es

https://orcid.org/0000-0002-9205-8458

Gianni Bartoli

Department of Civil and Environmental Engineering.

University of Florence, Florence I-50139, Italy

Email: gianni.bartoli@unifi.it

http://orcid.org/0000-0002-5536-3269

ABSTRACT

Recent years have seen a growing interest toward implementation and testing of structural health monitoring techniques for cultural heritage structures, and many scientific papers report on the application of operational modal strategies as an effective knowledge-based tool for vulnerability reduction of masonry buildings. Focusing on historic masonry bell-towers, being such structures particularly prone to earthquake-induced damage, the most part of the studies discuss structural monitoring and vibration-based identification methods with the goal of their seismic protection. As a consequence, while there is great number of researches that investigate masonry towers behaviour under earthquake loads, only a few scientific papers discuss their structural response under service loads such as bell-loads. This issue is also of paramount importance, since in many real cases the bell-ringing has been stopped due to the dynamic interaction phenomena that are activate between the bells and the host structure. With the aim to contribute of improving the knowledge in this field, this paper focuses on a methodology for the study of the dynamic interaction between bells and slender masonry towers. The proposed methodology is divided into four phases: (i) Geometric and structural characterization of the tower and bells; (ii) Evaluation of the dynamic forces generated by the swinging bells; (iii) Experimental campaign to characterize the dynamic properties of the tower by means of operational modal analysis; (iv) Parametric finite element analysis. To illustrate the methodology, a real case of masonry bell-tower in which bell-ringing had to be stopped due to a history of strong vibrations is discussed. The paper includes a method of analysing the dynamic properties of masonry bell-towers, in which the dynamic interaction between the harmonic bell forces and the fundamental tower modes is analysed by means of a calibrated numerical model and the dynamic amplification factor.

KEYWORDS:

Bells swinging; Operational modal analysis (OMA); Dynamic monitoring; Slender towers; System identification; Genetic algorithm (GA); Heritage preservation.

1. Introduction

Masonry bell-towers are a Cultural Heritage (CH) building typology widespread on the European territory whose preservation is a fundamental issue for modern societies since they represent an important cultural and economic asset. Being masonry towers, due to their specific structural configuration, particularly prone to earthquake-induced damage, last decades have seen a growing interest toward the application and setting-up of Structural Health Monitoring (SHM) techniques for their seismic protection, vulnerability reduction and damage assessment [1–5]. Today, hence, the scientific literature counts a remarkable number of researches investigating Ambient Vibration Tests (AVT), Operational Modal Analysis (OMA) and, more in general, vibration-based SHM methods for seismic protection of slender masonry towers (e.g. [6–9]). However, even if conservation against exceptional loads such as earthquakes is a relevant and pivotal issue (e.g. [10–12]), of paramount importance is also the characterization of masonry bell-towers behaviour under service loads such as the ones transferred by the ringing of the bells. This issue still represents a scientific and technical challenge, and in many real cases the bell-ringing has been stopped due to the dynamic interaction phenomena that are activate between the bells and the host masonry structure.

The dynamic loads to which bell-towers are subjected when the bells are rung depend on the way in which they are swung. In Europe, it is generally possible to distinguish three main types of swing: the English, Spanish, and Central European systems ([13]). In the English system, the bells describe a complete circle (360º), changing the swing direction in each cycle. In the Spanish system, the bells are usually fixed to the window frames, are provided with heavy counterweights and the bells rotate continuously in the same direction. In the Central European system, the bells are swung around their axes through an angle that can vary from 55º to 160º. Compared with the Spanish system, the English and the Central European systems are significantly out-of-balance and rest on specially designed bell-frames inside the towers ([13,14]). In fact, in the Central European and English systems, the bell yokes are no more than the bell support, while in the Spanish system bell yokes tend to be heavy and act as counterweights, thus allowing out-of-balance values of only 2-11 cm ([14]).

Knowledge of the time-dependent loads induced by the swinging of the bells is of major importance in the design, rapair or restoration of bell-towers ([15,16]). Depending on their angular velocity and their unbalance, these forces can in fact induce considerable dynamic interactions with the supporting structure ([15–19]). The first study that used the equations of motion to describe the bell's swinging was made in the19th century by Veltmann ([20,21]), who proposed a simple analytical model based on the equations of motion of a double physical pendulum to explain the failure of the Emperor's Bell in Cologne Cathedral. Almost a century later, Heyman and Threlfall ([22]) employed a similar double pendulum model to estimate the inertia forces induced by the bells. Also worthy of mention are the studies carried out by Majer & Niederwanger ([23]) and Wölfel and Schalk ([24]) in Germany, and Bennati et al. ([18,25]) in Italy. Müller ([26]) and Steiner ([27]), in particular, described the dynamic loads caused by the interactions between bells and bell-towers in the Central European system. Their work was continued by Schütz ([28]) and by the authors of the German DIN 4178 standard ([29,30]), who developed a semi-empirical description of the forces acting on the bells' supports. Similar studies were performed on the English system by Wilson and Selby ([31,32]), who measured the effects of the dynamic forces generated by swinging bells. The Spanish system was investigated in depth by Ivorra et al. ([14], [33]), who studied the influence of the mounting on the dynamic reaction forces produced by swinging bells by means of numerical simulations and laboratory tests. They compared the three types of mounting and found that the Spanish system transmitted significantly lower forces than the English and Central European ones. The different approaches are able to provide the vertical and horizontal forces involved in bell ringing. From the different tests performed, it can be said that the most important bell characteristics are: imbalance, turning speed, inertia and weight).

With the aim to contribute of improving the knowledge on the dynamic interaction between the harmonic bell forces and the fundamental modes of the tower, this paper presents a methodology discussed through a real CH case study: the historic Fiesole's Cathedral bell-tower near Florence (Italy). The tower dating from the Middle Ages, represents an elucidating case study because: i) due to its slenderness, it had a history of perceived strong vibrations when the bells were rung that concluded with the stop of the bell-ringing to avoid structural damage; and ii) not being an isolated structure (at the lower levels the tower is incorporated in the confining church structure) several issues arise concerning the actual degree of confinement offered by the surrounding structures that can be generalized for similar structures.

The paper is organised as follows. First, a brief description of the characteristics of the masonry bell-tower considered is given. Second, the dynamic forces due to the swinging bell are described, taking into account the swing angle and the harmonics of the horizontal bell loads. Third, experimental vibration tests performed to characterize the dynamic properties of the tower by means of Operation Modal Analysis (OMA) [34,35] are reported, including the damping factor and the tower's natural frequencies due to in-situ environmental and bell swinging forces. Eventually, numerical parametric analyses are employed to investigate the dynamic interaction phenomena between bells and tower: firstly, a numerical finite element (FE) model is updated by Genetic Algorithm (GA) techniques [36], together with a sensitivity analysis of the effect of lateral wall stiffness on the tower's main frequencies and modal shapes; secondly the interaction between the harmonic bell forces and the tower's modal shapes is analysed. The parametric analysis includes the lateral confinement of the tower due to wall stiffness, the velocity and swing angle of the bells, and the position and direction of the bell forces.

The paper includes a method of analysing the dynamic properties of masonry bell-towers, in which the dynamic interaction between the harmonic bell forces and the fundamental tower modes is analysed by means of a calibrated numerical model and the dynamic amplification factor (DAF) proposed in DIN 4178. The results here obtained can be extrapolated to similar types of slender structures and highlight the effect of the harmonic bell forces on the error obtained between the real dynamic response and the one proposed in the German DIN 4178-1978 and DIN 4178-2005 standards.

2. Methodology

2.1. Description of the slender masonry bell-tower

The medieval bell-tower selected for this study is on the north side of the Cathedral of Fiesole (Italy) and has a rectangular cross section with an external side of about 5.10 x 4.10 m, with an overall height of about 40 m. Three principal elements can be identified. The first element (from 0 m to 26.30 m) represents the basement which has three different transversal sections according to the exterior wall thickness: *i*) from 0 m to 7.25 m the thickness is 1 m, *ii*) from 7.25 m to 22.15 m the thickness is 0.85 m, and *iii*) from 22.15 m to 26.30 m the thickness is 0.75 m. The basement has no windows, except for a small window at 22.15 m. At the base of the tower two large arched openings allow access from the lateral church. The second element (from 26.30 m to 38 m) represents the belfry, which has a constant wall thickness of 0.75 m and two types of openings at bell height: *i*) the first, at 26.30 m, has one opening per wall (single lancet window) at the level of the smaller bells; *ii*) the second, at 30.90 m, has two mullioned windows on each wall. Only the biggest bell is located at this level, in the centre of the tower. The third element (from 38 m to 39.65 m) is the crown, with 0.25 m thick battlements typical of medieval towers.

It should be noted that there are two floors inside the tower: one at 15.50 m and another at 26.50 m. These floors are formed by groin vaults joined to the lateral walls and improve their torsional stiffness. It is also important to note that the bell tower is connected to the lateral walls of the main body of the cathedral on the north, south and west sides (**Fig. 1**). The thickness of these lateral walls is about 1 m. The materials used to build the tower, from 0 to 26.30 m, are irregular stone blocks with thick layers of mortar. From 26.30 m to the top, the material is of regular stone blocks. In this study, all the materials are considered as irregular stone blocks with mortar, according to the Italian Recommendations ([37]).

The tower contains four historical bells at a height of 26.60 m: “*Fratina*”, “*Cantina*”, “*Misericordia*” and “*Linara*” (**Fig. 2** and **Fig. 3)**. “*Cantina*” is the smallest of the bells with a weight of 2.256 kN, while “*Fratina*”, “*Misericordia*” and “*Linara*” weigh 2.452 kN, 3.237 kN and 4.395 kN, respectively. The largest bell, “*Campanone*”, at 30.90 m in the centre of the belfry, moves in the east-west direction and weighs 7.142 kN.

2.2. Dynamic bell forces

The bells in this tower rotate according to the Central European System defined in Ivorra et al. ([38]). The bell oscillation around the horizontal axis introduces dynamic forces due to the inertia accelerations of the bell mass. These inertial forces depend on the mass of the bells, m, the position of the centre of gravity in relation to the oscillation axis, s, the bell inertia, I, and the swing velocity (**Fig. 2**). These parameters are related to each other by means of the geometry coefficient, c, **Eq (1),** and can be approximately evaluated by DIN4178 ([29,30]) and taking into account the information provided by Heyman and Threlfall ([22]) and Ivorra et al. ([33]). The dynamic and static properties of the bells are summarised in **Table 1**. The swing rotation angle and swing velocity are the normal values calculated for these bells according DIN4178.

$$c = \frac{m \cdot s^2}{I + m \cdot s^2} \tag{1}$$

$$H(t) = c \cdot (m \cdot 9.81) \cdot \sum \gamma \cdot \sin(\Omega_i \cdot t) \tag{2}$$

The dynamic bell forces can be divided into two components: horizontal, $H(t)$, and vertical $V(t)$ ([38]). The vertical forces are usually neglected, as the axial stiffness of masonry towers is higher than their bending stiffness, so that no resonance problems are expected. Horizontal forces can be evaluated according to the simplified expression contained in **Eq. (2)** for the Central European bell-ringing system [22]. These equations consider the swing velocity, Ω, and the swing rotation angle effect, α (**Fig. 2**) by means of the γ coefficient. The horizontal forces are transferred to the tower and can induce horizontal movements that threaten its structural integrity ([15,38]).

Table 1 shows the bells’ maximum horizontal dynamic forces, evaluated without taking into account the dynamic amplification due to the bell-tower displacement interaction, which is related to the harmonic frequencies of the horizontal bell forces and the vibration frequencies of the tower, which can generate amplification problems when the frequencies are close to each other.

To evaluate the effect of the bell swing rotation angle on the harmonic frequencies and the horizontal force, (**Fig. 4**) shows an example of *Campanone’s* dynamic horizontal forces and the Fast Fourier Transform (FFT) analysis of these forces for two possible swing rotation angles: 64º and 160º. When the swing rotation angle is 64º (a common value for this type of bell) the first harmonic produces the highest force. The second and third produce 0.725 and 0.1 of the first harmonic horizontal bell forces, respectively. When the swing rotation angle is 160º the effect of the first horizontal bell harmonic force is 6 times smaller than the second and third harmonic forces, while for the same bell swing velocity, the total horizontal force for this swing rotation angle is three times higher than for α equal to 64º.

This confirms the importance of controlling the swing velocity and the swing rotation angle in order to avoid possible interactions problems between the bell harmonics and the fundamental bell tower modes.

2.3. Experimental test

To perform the dynamic test on the tower, six 393C PCB Piezotronics uniaxial accelerometers were placed at a height of 30.9 m (accelerometers 1, 2 and 3) and 38 m (4, 5 and 6) on the tower's inner east wall in a triaxial configuration to record horizontal (accelerometers 2, 3, 5, 6) and vertical (1 and 2) accelerations. These devices were fixed by screws to a steel girder to ensure their orthogonality. Tower vibrations were measured with this test setup, the E-W (ZX bending plane, accelerometers 3 and 6) and N-S (ZY bending plane, accelerometers 2 and 5). The measurement range of these accelerometers is between 0.025 Hz to 800 Hz, with a voltage sensitivity of 1000 mV/g. Data acquisition hardware consisted of one PCB 482A22 signal conditioner and one HBM Spider8 (SR55) data logger. The data acquisition was carried out at a sampling frequency of 400 Hz.

The experimental test was divided into two phases, according to the external dynamic loads. The first phase consisted of three records of about 5 minutes excited by means of ambient noise. The second phase was divided into two types of dynamic load. Two manual impulses were applied to the top of the tower in the E-W direction and another two in the N-S direction. Another 6-minute recording was done while swinging "*Misericordia"* in the East-West direction at a swing rotation angle of 100º and a swing velocity approximately equal to 30 rev/min.

In the signal post-processing of the ambient vibrations test, the signals were first decimated by a factor of 8 to obtain a frequency of 50 Hz and were then filtered between 0.1 and 20 Hz. With the aim to avoid aliasing issues an anti-aliasing filter 8th order Chebyshev Type 1 low pass filter was used. Operational Modal Analysis (OMA) was then used to evaluate the principal frequencies and damping factors of the first five tower vibration modes [39]. Regarding the frequency domain identification, the techniques used for this purpose were: Frequency Domain Decomposition (FDD), Enhanced Frequency Domain Decomposition (EFDD), Curve-fit Frequency Domain Decomposition

(CFDD) . Regarding the time domain identification, the techniques used were: Unweighted Principal Component (UPC), Principal Component (PC), and Canonical Variate Analysis (CVA). The last three techniques belong to the Stochastic Subspace Identification (SSI) family.
The signals registered in the forced vibration test were filtered between 0.1 to 20Hz [40].

2.4. Numerical Parametric study of the tower

Two different numerical models were used to evaluate bell-tower interaction and the effect of lateral restraint on the dynamic interaction. The first consisted of the tower without any lateral constraint and the second was the tower with lateral constraining walls. ANSYS commercial code with solid elements was adopted to build the numerical models. A perfect bonded condition was assumed between tower and walls in the second model.

2.4.1. Numerical model updating

An optimization procedure was used to calibrate the elastic properties of the numerical model by means of Genetic Algorithm (GA) techniques ([36,41]). The mechanical properties selected for this process were: the elastic modulus of the lateral walls (Ew_1, Ew_2, Ew_3), the bell-tower's elastic modulus (E_{t1}), and the self-weight of the masonry (ρ_{t1}).
A population of 20 chromosomes with a uniform random distribution was used. Stochastic uniform and single point procedures were the selector operator and crossover technique, respectively. Values of 10% and 80% of the initial population were selected for the elite count and crossover fraction. An adaptive feasible option and 75 generations were selected for the mutation technique and number of generations, respectively. The relative errors between the experimental and numerical modal frequencies were used as fitness functions for the first five natural frequencies. **Table 2** shows the usual range of values for the variables analysed in similar studies. According to these it is possible to set the possible range of the expected values for the equivalent elastic modulus, E, and the self-weight, ϒ, between 1100 and 2500 MPa for elastic modulus, and between 16-19 kN/m³ for self-weight. Random upper and lower elastic modulus limits of 1.2E3-1.2E5 MPa were selected for the lateral walls with the aim to avoid problems related to local minimums solution during the optimization procedure.

2.4.2. Effect of tower confinement.

After the model updating procedure, the results related to the optimal elastic modulus of confinement walls showed a high variation coefficient. With the aim to evaluate the real effect of the lateral walls in the tower vibration modes and modal shapes, and to control the results evaluated by means of GA.

A parametric analysis has been performed changing the lateral walls stiffness. In particular, the numerical values and the modal shapes of the tower vibration modes were analysed for different values of lateral wall stiffness, ranging from 0 (non-confined tower) to the optimal value reached by means of the GA (confined tower). 201 models were evaluated, increasing the elastic modulus of the lateral walls by 0.5% of the expected optimum value each time.

2.4.3. Effect of the bell and tower dynamic interaction

The main problem involved in swinging bells is the possible interaction between the bell and tower frequencies. To evaluate this condition, the analysis was divided into two phases: in the first, a parametric analysis considered the bell's swing velocity, its harmonic component, Ω_i, and the tower's vibration frequencies, ω_j. The dynamic amplification factor, DAF, was then evaluated according to **Eq. (3)**:

$$DAF_{ij} = \frac{1}{\sqrt{\left(1-\left(\frac{\Omega_i}{\omega_j}\right)^2\right)^2 + \left(2\cdot\xi\cdot\frac{\Omega_i}{\omega_j}\right)^2}} \tag{3}$$

It is important to note that the damping factor considered was equal to 1.5%, according to the experimental results and the values proposed in DIN4178 ([30]). The swing velocity range was selected from the most usual values used for bell towers.

In the second phase the dynamic interaction was evaluated between the previously selected bell resonant swing velocity and the real tower, and included a new parametric analysis. Three new variables were introduced in the analysis: the first was bell swing angle, φ, the second the position of the bell force, with two possibilities according the actual position of the bells, the third was the direction of the bell force, with two possibilities according to the actual direction of the bells (**Fig. 2**). The output variables, the maximum displacement and velocity at the plane of the floor of the uppermost full storey, were analysed. In each case, the maximum value in the X or Y direction and its concomitant value in the perpendicular direction at the same time were evaluated at the central point of the upper floor and the SRSS value of these directions was used as the resulting value. **Table 3** gives a summary of the input and output parameters used during the parametric analysis.

To study possible damage to the bell-tower due to the dynamic interaction between bells and tower, the [42] standard was considered. In this case, the maximum velocity on the floor plane of the uppermost full storey for all frequencies should be less than 8 mm/s. This value is higher than the 3 mm/s proposed in DIN 4178. If the numerical model shows higher velocity values, these values can ensure a higher damage level.

2.4.4. Efficiency evaluation of the equations proposed in DIN 4178.

The last part of the study was related to the methodology proposed by DIN 4178 to evaluate the maximum displacement of the tower by means of static equivalent forces, considering the dynamic interaction between bells and tower. There are two current versions of this standard, the older, from 1978 to 2005, shows that the static equivalent force can be evaluated as the maximum value reached by means of **Eq. (4)**:

$$H_s(t)_{DIN\ 4178-1978} = c \cdot (m \cdot 9.81) \cdot \sum \gamma_i \cdot DAF_i \cdot \sin(\Omega_i \cdot t) \qquad (4)$$

In this case, the DAF factor, **Eq. (3),** is estimated by taking ω_j as the first principal tower vibration frequency in each direction. It should be noted that the DAF was evaluated in a different way to that described in Section 2.4.3, in which the first five frequencies of the tower in each direction were considered, while only the first frequency in each direction was considered in 2.4.4, according to the previous standard. This is due to the fact that DIN 4178 considers only the interaction of the bell harmonics with the tower's first vibration mode. In 2005 a new version of DIN 4178 was published, in which the equivalent horizontal forces could be evaluated in the same way as in the 1978 version, but using **Eq. (5)**:

$$H_s(t)_{DIN\ 4178-2005} = 1.1 \cdot c \cdot (m \cdot 9.81) \cdot \sum \gamma_i \cdot DAF_i \cdot \operatorname{sign}\left(1 - \frac{\Omega_i}{\omega_0}\right) \sin(\Omega \cdot t) \qquad (5)$$

Two principal differences were introduced, the first was the safety factor of 1.1, which allowed for the uncertainty of the method. The second was the $sign$ function, which is used to consider the interaction between the movement directions of the bell and the tower. In **Eq. (5)**, ω_0 is the first frequency of the tower in each direction.

The aim here was to evaluate the influence of bell harmonics on the structure response according to DIN 4178, especially the relative error between the exact and simplified solutions. **Table 3** gives the input and output parameters used during the parametric analysis.

3. Results and discussion

3.1. Bell tower dynamic properties.

Table 4 gives the first five frequencies for the ambient test according to the different techniques used. The overall mean frequencies for the first bending modes in ZX and ZY directions are 0.87 Hz and 0.98 Hz, respectively. The second bending modes in both directions are 3.97 Hz and 4.46 Hz, respectively. No vertical mode results were evaluated due to the high noise detected in the vertical signals (accelerometers 1 and 4) [1,3]. The torsional mode identified is related to the frequency of 3.55 Hz. The modal damping evaluated during these tests shows a mean value for all the techniques equal to 1.63%, 1.42%, 1.66%, 1.93% and 1.37% from mode 1 to mode 5, respectively. The acceleration level for these damping values is between 0.5E-3 to 1.5E-3 m/s². These damping factor values are very similar to the one proposed by DIN 4178, i.e. equal to 1.5% for masonry buildings.

Regarding the results for the forced vibration test, in the case of manual load, the acceleration level registered is similar to the ambient test, showing that this type of load is not significant enough to increase the acceleration level even in this slender tower. For swinging bell loads, the peak acceleration level registered is 0.018 m/s² (**Fig. 5**). In this case, the global damping factor in the swing direction is 1.5%. It is worth noting that for a peak acceleration twenty times higher than the ambient test, the damping factor remains constant between 1.5 % and 2 %. On the other hand, the dynamic interaction between the bell and the tower, **Fig. 5** shows the results of the FFT analysis of the signal, in which the first and second tower bending frequencies in E-W direction, 0.98 Hz and 4.47 Hz, and the first, 0.5 Hz, and the third, 1.5 Hz, bell harmonics were identified. These results show that the distance between the first bending mode and the first and third bell harmonics is higher than the limitation of 20% proposed by DIN 4178, indicating that no serious resonance problems were detected during the test.

3.2. Effect of tower confinement and modal updating.

Table 5 gives the updated elastic properties, the initial range value and the standard deviations (in brackets) of all the elements obtained by means of the GA after 3 runs. The optimized frequencies, with a global error equal to 3.31%, are: 0.81 Hz, 0.99 Hz, 3.68 Hz, 4.03 Hz and 4.67 Hz. Table 4 shows the numerical and experimental frequencies and the MAC values (Modal assurance criterion). These values show that the vibration frequencies and modal shapes between the numerical and experimental results are very close, and then, the dynamic solution of the elastic-linear problem, will be well conditioned. In this way it is possible to apply simplified boundary conditions instead of modeling the entire adjacent structure". Some examples are [43], [44] and [38]. To evaluate the calibrated parameters in the time domain, the real and the numerical response of the tower for the experimental test were compared (**Fig. 5**), the results of which verified the calibration of the finite element (FE) model in the time and frequency domains [45].

The GA results show low standard deviation values for the main tower's elastic properties, E_{t1}, ρ_{t1}. However, the lateral walls, E_{w1}, E_{w2} and E_{w3} have high values (56%, 21% and 67%). **Fig. 6** gives the relationship between the lateral stiffness of the walls and the vibration frequencies of the tower, which can explain this behaviour. In **Fig. 6**, f_i is the frequency of the tower for the lateral stiffness selected, f_{max} is the optimized frequency obtained by the GA, E_i is the lateral stiffness selected and E_{max} is the optimized lateral stiffness obtained by the GA. It is important to note that for the first bending mode in X or Y direction, only a value between 2% and 3% of the GA proposed value is necessary to reach 90% of the optimum frequency value. Moreover, for the second mode in both directions, only a value of 5% of the proposed GA value is necessary to reach the same proportion of the optimal value. These results show that an elastic modulus equal to 5839 MPa, 3375 MPa and 5970 MPa for E_{w1}, E_{w2}, and E_{w3}, respectively, are enough to optimize the bending modes, and then the normal elastic modulus can be used to model the lateral walls. It should be noted that for values above 10% of the relative lateral stiffness, the curve is practically horizontal for the bending modes, and for this reason a wide range of values optimize the frequency results of the GA method.

However, the real problem during the optimization process is found in the torsional mode. In this case, a higher value is necessary to reach the optimal torsional frequency (**Fig. 6),** due to the fact that the simplified model does not take into consideration all the real torsional restraints. **Fig. 7** and **Fig. 8** show the modal shapes and frequency values for zero lateral stiffness and for the minimum lateral stiffness value necessary to reach 90% of the torsional frequency value.

The parametric analysis shows that the best solution for the modal analysis is reached by considering the lateral walls as fixed supports or as having very high lateral stiffness. These results are consistent with the semi empirical formulation proposed by Bartoli et al. ([46]), who evaluated the first vibration frequency considering the effective height of the tower, or the part of the tower above the lateral walls. The numerical results obtained in this research show that it is advisable to use the effective tower height to evaluate the higher vibration frequencies.

3.3. Dynamic interaction between bells and bell tower.

Fig. 9 shows the results of the first parametric analysis aaccording to Section 2.4.3. In this figure it is possible to analyse the relationship between the main velocity of the bell and the interaction between its harmonics and the tower vibration modes. It should be noted that in this analysis the problem was analysed as a single degree of freedom, without taking into account the bell position or the bell swing angle.

Fig. 9 shows that a bell velocity of 19.8 rev/min gives a dynamic interaction between the third harmonic of the bell (3ºH) and the second mode of the tower (M2). Velocities equal to 24.53 rev/min, 31.54 rev/min, 44.15 rev/min have dynamic interactions between the 9th, 7th and 5th bell harmonic, respectively, and the 3rd mode of the tower. Velocities of 26.87 rev/min and 34.54 rev/min have dynamic interactions between the 9th and 7th bell harmonic with the 4th tower vibration mode.

Velocities of 31.2 rev/min and 40.11 rev/min give a dynamic interaction between the 9th and 7th bell harmonic with the 5th mode of the tower.

According to these results, the critical velocities were selected for the second phase of the parametric analysis (Section 2.4.3). These selected bell swing velocities show a dynamic interaction not only with the first or second mode, but also with higher modes. According to **Fig. 4**, the effect of the bells' harmonics on the dynamic bell forces change with the swing angle. Since the real structural response is a combination of dynamic interaction and bell harmonics, a multi degree of freedom model (FE model) was analysed.

Fig. 10 shows the normalized velocity of the tower response for different velocities, swing angles, heights and swing directions of the bell's dynamic loads. This figure can be used to evaluate the dynamic effect of any bell by multiplying the normalized value by the F factor, **Eq. (6)**. Where c^* and w^* are the geometry coefficient and weight of the real bell in N. In this figure it is also possible to evaluate critical or non-critical situations from the point of view of damage to the structure, according to DIN4150 (or other standards) [47]. In these cases it is necessary to divide the standard velocity limitation by the F factor. **Fig. 10** shows the velocity limitation for DIN4150 and for each of the bells in the tower by a horizontal dashed line. The directions of the selected bells' limitations are equal to the bells' real directions ("*Fratina*" and "*Misericordia*" in E-W direction and "*Cantina*" and "*Linara*" in N-S direction). However, to take into consideration the effect of different bell masses, in addition to the real bells, the limitation of the bells was included in different directions and heights. For example, "*Campanone*" was evaluated at heights of 30.9 m and 26.3 m.

$$F = c^* \cdot \frac{w^*}{1000} \tag{6}$$

The results show that the tower's worst load case is when the bells are at 30.9 m, swinging at 19.8 rpm with a swing angle of 140º and a maximum normalized velocity of the building equal to 33.09 mm/s. This critical situation is also found when the bells swing at 26.3 m, even when the swing direction is perpendicular to the movement of the tower (**Fig. 10)**. According to DIN4150, all the bells could cause structural damage to the tower at this bell swing velocity. In all these cases the FFT analysis of these signals shows a resonance between the second tower mode, with maximum displacement in the X direction and the third bell harmonic.

At other bell swing velocities the dynamic interaction with the principal bending mode is lower than 19.8 rpm. In these cases swing angle is an important factor in determining whether the standard limitations have or have not been reached. For example, with a swing angle less than 50º all the bells can swing at any velocity, height or direction. When the dynamic interaction is close to the higher bell harmonics, the peak of the structural response occurs at greater bell swing angles.

Three points should be highlighted here; the first is the dynamic interaction between the bell harmonics and the tower's first or second vibration frequency when their frequencies are different, for example, the results for 24.53 rpm, 26.87 rpm, 31.2 rpm and 31.54 rpm, with a third harmonic of 1.23 Hz, 1.34 Hz, 1.56 Hz and 1.58 Hz. In these cases, the third bell harmonic is 20% higher than the second frequency of the tower, 0.99 Hz, as recommended in DIN4178. However, **Fig. 10** shows that these velocities exceed the limit value at different swing angle ranges. Furthermore, for 31.2 rpm and 31.54 rpm and the bell at 26.3 m, the shape of the final section of the curve with a swing angle ranging from 150º to 170º, is more horizontal than the other curves due to the dynamic interaction between the ninth harmonic and the fifth mode of the tower.

The second point is related to the torsional modes; the FFT analysis of the signals did not find any dynamic amplification between these and the bells' harmonics, possibly due to the position of the control point close to the torsional axis.

The third point concerns bell swing velocities of 40.11 rpm and 44.15 rpm with bells at 26.3 m and 30.9 m. **Fig. 9** and **Fig. 10** show the dynamic interaction between the seventh bell harmonic and the fifth tower mode at 26.3 m for both velocities and between the first bell harmonic and the first tower mode at 30.9 m and 26.3 m at 44.15 rpm. It should be noted that the dynamic interaction with the seventh bell harmonic only appears when the bells are at 26.3 m, due to the tower's fifth modal shape having a displacement value close to zero at 30.9 m. This behaviour is directly related to the effect of lateral wall stiffness on the effective height of the tower. Regarding the damage evaluation, a bell swing velocity of 40.11 only shows problems at 26.3 m in both directions. At 44.15 rpm, problems are found at 30.9 m at bell swing angles from 50º to 110º in the E-W direction and at 26.3 m at angles from 50º to 170º.

Finally, it is important to note that bells similar to "*Misericordia"* and "*Linara"* can be found in many masonry bell towers. "*Misericordia"* showed potential damage problems at a velocity of 19.8 rpm and all swing angles. However, at swing velocities higher than 26.87 rpm no problems were found for any direction, location or swing angle, while "*Linara"* was more restricted by swing velocity limitations. These results show that when there is a dynamic interaction between bell and tower, a slight variation of the bell mass or a slight variation of the geometry coefficient c, can avoid resonance problems better than changing the bell swing velocity range. The c coefficient can be changed by using a counterweight or changing the geometry of the bell yoke ([13,16]).

3.4. Evaluation of global DAF factor by means of DIN4178.

The analysis of the error between the static and dynamic response by means of DIN4178 and the FE model was evaluated according to Section 2.4.4. To analyse the effect of the dynamic amplification of the structure's response **Fig. 11** shows the relationship between the dynamic and the static tower displacements. In this case the static load was evaluated by **Eq. (4)** proposed in DIN4178-1978**,** but taking the DAF value as 1 for all the bell harmonics. In this way the static load is not affected by the dynamic interaction. In general, DAF values higher than 1 indicate that the dynamic interaction increases the static load, while values lower than 1 indicate that the interaction between the swing harmonics and bell tower vibration modes reduces static load. DAF values equal to 1 indicate the absence of a dynamic interaction. The results shown in **Fig. 11** can be divided into three different cases that are similar for all the locations and directions analysed:

a) Swing velocity of 19.8 rpm; this case shows a DAF value higher than 1 for all swing angles. The maximum DAF value is for a different swing angle than for the maximum velocity (**Fig. 10**). **Fig. 11** shows a maximum value for 110º instead of 140º. These results mean that at this swing angle and swing velocity the bell and tower dynamic interaction reduces the effect of the higher bell harmonics;

b) Swing velocities of 44.15, 40.11, 34.54, 31.54 and 31.2 rpm; in these cases, with swing angles from 50º to 110º-130º, the structural response shows a dynamic interaction between the first bell harmonic and the first tower mode, after which the DAF value is higher than 1. This dynamic interaction only appears in the first few seconds of vibration, and is due to the effect of the transient component of the structural response. Another result is related to the decrease in the DAF factor when the swing angle increases. Due to the higher swing angle values, the effect of the first bell harmonic is reduced. From 110º-130º to 170º the DAF value is lower than 1, which means that the dynamic interaction reduces the high harmonic forces. At these swing angles, the first harmonic static force of the bell drops to zero but the static force of the higher bell harmonics increases with the swing angle. This behaviour, together with the dynamic interaction effect, reduces the DAF value to below 1.

c) Swing velocities of 24.53 and 26.87 rpm; these cases show a similar behaviour to that for 19.8 rpm, but with lower dynamic interaction. For this reason the maximum DAF value are close to the swing angles, where the dynamic interaction is higher than the effect of the harmonic forces, for example, swing angles of 80º and 130º for the first and third harmonic bell forces (**Fig. 11**).

To analyse the relative error between the real structural response and that proposed by DIN4178, **Fig. 12** and **Fig. 13** show this value according to the standards published in 1978 and 2005, respectively.

For DIN4178-1978 and swing velocity of 19.8 rpm the relative error varies from 13% to 16% in the X direction and both bell locations. For the Y direction the value varies from -40% to -62.8%. This negative deviation is due to considering the tower vibration mode associated with the bell force direction. This means that for the analysis in the Y direction, the principal frequency in **Eq. (3)** is 0.808 Hz and 0.99 Hz for the X direction. In this case, where the dynamic amplification is at 0.99 Hz for the third harmonic bell force, safer results could be obtained using 0.99 Hz as the principal frequency instead of 0.808 Hz. Using this value, the relative error ranges from +431% to 463%.

For DIN4178-2005 and the same swing velocity the results show a relative error close to -100% in the X direction. These results are due to the function $sign$ taking values of 0 for cases with $\frac{\Omega_i}{\omega_0}$equal to 1. In the Y direction, the combined effect of the $sign$ function and the security factor equal to 1.1 (**Eq. (6))**, reduces the relative error, especially for swing angles from 50º to 80º. However, all the results for this swing velocity are negative, even if the principal frequency used in **Eq. (6)** is 0.99 Hz instead of 0.808 Hz. This indicates that the results obtained by the two standard versions are unsafe for this case in which the dynamic interaction is between the tower's mode 2 and the third bell harmonic.

When swing velocity is 44.15 rpm according the 1978 standard version, the dynamic interaction is between the first tower mode and the first bell harmonic force (**Fig. 9**). The relative error is close to -50% for the analysis in the X direction (w_0=0.99 Hz). This error is due to the dynamic amplification during the transient period of the tower movement. However, as with a swing velocity of 19.8 rpm, if a $w_0$of 0.808 Hz is used for the X direction instead of 0.99Hz, the relative error changes to a value close to +35%. In the Y direction analysis the relative error is close to -35%.

Both the 44.15 rpm and the 19.8 rpm results show that in cases where the directions of the bell forces are not in the direction of the tower's resonant mode with the first or third bell harmonic, it is better to consider the resonance frequency of the tower as w_0 instead of the vibration mode parallel to the bell force direction.

Positive results similar to those of DIN4178-1978 were obtained for the solutions proposed by DIN4178-2005 for 44.15 rpm. In this case, where the coefficient $\frac{\Omega_i}{\omega_0}$is close to but not exactly equal to one, the $sign$ function changes the slope of the relative error curve and better results were obtained for higher swing angle values. It is important to note that after these positive results reach a peak value, the slope of the relative error curve descends and the negative results increase (**Fig. 13**) in both standard versions due to the reduced dynamic interaction between the first bell harmonic and the tower's first vibration mode. In other words, the equations proposed in DIN4178 give relatively good results when the tower displacement due to the bell being rung is similar to a sine function. However, when the combination of harmonic forces moves the tower asymmetrically then the relative error obtained from the equations proposed by the standards increases sharply. It should be noted that this situation usually happens during the transient state of the tower movement, and that the maximum swing angle of the bell at which the slope of the relative error descends is reduced as the dynamic interaction decreases (**Fig. 13**).

The results obtained for the other swing velocities show that the tower behaves similarly to the case of 44.15 rpm.

4. Concluding remarks

This paper proposes a methodology for the parametric study of the dynamic interaction between bells and slender masonry towers, involving a case study with an experimental and numerical evaluation of the dynamic interaction. The experimental analysis was carried out by means of ambient and forced tests with swinging bells. When the results of both tests were evaluated by means of OMA techniques it was found that the main frequencies of the tower are very close to the swing velocities commonly used in historical bell towers. A global damping factor close to 1.5% was experimentally detected.

The numerical analysis was performed on an FE model of the tower calibrated by GA techniques, considering the elastic modulus of the confining lateral walls and the elastic modulus and self-weight of the masonry tower elements as calibration variables. The results indicated similar behaviour in the frequency and time domains between the numerical and experimental results. However, a high variation coefficient was obtained for the elastic modules of the lateral walls by the model updating process. A parametric analysis was also performed to evaluate the relationship between the stiffness of the lateral walls and the main tower frequencies. The results of the bending modes show that lateral stiffness values of less than 5% of those obtained from Genetic Algorithm techniques are enough to obtain a relative error of less than 10% between the experimental and numerical frequencies, although a higher lateral stiffness value is necessary to reach the same relative error for torsional modes. The numerical results show that for a confined tower the best results can be achieved by using perfect lateral constraints instead of equivalent lateral walls.

The parametric analysis of the dynamic interaction between the tower and the bells assumed swing angles, velocities, position and direction of the bells as parametric variables. The results were obtained for a normalized bell so that they could be applied to any bell by means of the normalized factor F. The DIN4150 restrictions for the tower movements were considered. The results show that in cases where the dynamic interaction was between the first or third bell harmonic and the first or second tower vibration frequencies, the horizontal displacement of the tower's highest level can induce damage to the structure, regardless of the swing angle. In these cases, the higher bell harmonics can be neglected and the movement at the top of the tower is closely similar to a sine wave. However, when the dynamic interaction decreases, the effect of the bell harmonics increases and the displacement at the top of the tower is less similar to a sine wave. In these cases, no resonance situations can exceed the recommended values proposed by DIN4150, especially during the transient state of the tower movement.

A parametric analysis of the displacements proposed by DIN4178 using the static equivalent forces was also performed on the relationship between the global amplification factor for dynamic and static loads. The results show a lower relative error for the 2005 DIN4178 version than for the 1978 version only if the relationship between the frequency of the first or third bell harmonic and the vibration frequency of the tower's first or second mode are other than one. The 2005 version shows a different positive slope for the relative error curve to the horizontal slope for the older version, due to the effect of the $sign$ function introduced in the new standard version to evaluate the effect of the harmonic force component direction on the static horizontal force. However, the slope of the relative error curve changes to negative values when the effect of the higher harmonics increases in the structural response, and the dynamic amplification decreases, especially during the transient state of the tower movement.

Finally, with the aim of improving the results achieved by using the equations proposed in the standards evaluated in this study, when the ratio between the first or third bell harmonic and the first or second tower vibration frequency is close to 1, it is recommended to use the tower vibration frequency as ω_0, which is similar to the harmonic frequency of the bell, regardless of the direction of swing, although the improvement is negligible when this ratio is not close to 1. It should be noted that for situations in which the bells do not produce a direct resonant interaction the indications of DIN4178 standard are unsafe.

Acknowledgements

The authors are grateful to the Spanish Ministry of Economy and Competitiveness, who partially supported this study by Grant BIA2015-69952-R and BES-2013-064068.

REFERENCES

[1] L.F. Ramos, R. Aguilar, P.B. Lourenço, S. Moreira, Dynamic structural health monitoring of Saint Torcato church, Mech. Syst. Signal Process. 35 (2013) 1–15.

[2] L.F. Ramos, L. Marques, P.B. Lourenço, G. De Roeck, A. Campos-Costa, J. Roque, Monitoring historical masonry structures with operational modal analysis: Two case studies, Mech. Syst. Signal Process. 24 (2010) 1291–1305.

[3] F. Lorenzoni, F. Casarin, M. Caldon, K. Islami, C. Modena, Uncertainty quantification in structural health monitoring: Applications on cultural heritage buildings, Mech. Syst. Signal Process. 66–67 (2016) 268–281.

[4] F. Ubertini, G. Comanducci, N. Cavalagli, A. Laura Pisello, A. Luigi Materazzi, F. Cotana, Environmental effects on natural frequencies of the San Pietro bell tower in Perugia, Italy, and their removal for structural performance assessment, Mech. Syst. Signal Process. 82 (2017) 307–322.

[5] F. Ubertini, N. Cavalagli, A. Kita, G. Comanducci, Assessment of a monumental masonry bell-tower after 2016 central Italy seismic sequence by long-term SHM, Bull. Earthq. Eng. 16 (2018) 775–801. doi:10.1007/s10518-017-0222-7.

[6] C. Gentile, A. Saisi, A. Cabboi, Structural identification of a masonry tower based on operational modal analysis, Int. J. Archit. Herit. (2015). doi:10.1080/15583058.2014.951792.

[7] A. Saisi, C. Gentile, Post-earthquake diagnostic investigation of a historic masonry tower, J. Cult. Herit. (2015). doi:10.1016/j.culher.2014.09.002.

[8] A. Cabboi, C. Gentile, A. Saisi, From continuous vibration monitoring to FEM-based damage assessment: Application on a stone-masonry tower, Constr. Build. Mater. (2017). doi:10.1016/j.conbuildmat.2017.08.160.

[9] N. Cavalagli, G. Comanducci, C. Gentile, M. Guidobaldi, A. Saisi, F. Ubertini, Detecting earthquake-induced damage in historic masonry towers using continuously monitored dynamic response-only data, Procedia Eng. 199 (2017) 3416–3421. doi:10.1016/j.proeng.2017.09.581.

[10] S. Casolo, G. Milani, G. Uva, C. Alessandri, Comparative seismic vulnerability analysis on ten masonry towers in the coastal Po Valley in Italy, Eng. Struct. 49 (2013) 465–490. doi:10.1016/j.engstruct.2012.11.033.

[11] G. Castellazzi, A.M. D'Altri, S. de Miranda, A. Chiozzi, A. Tralli, Numerical insights on the seismic behavior of a nonisolated historical masonry tower, Bull. Earthq. Eng. 16 (2018)

933–961.
[12] G. Bartoli, M. Betti, A. Vignoli, A numerical study on seismic risk assessment of historic masonry towers: a case study in San Gimignano, Bull. Earthq. Eng. 14 (2016) 1475–1518. doi:10.1007/s10518-016-9892-9.
[13] S. Ivorra, F.J. Pallarés, Dynamic investigations on a masonry bell tower, Eng. Struct. 28 (2006). doi:10.1016/j.engstruct.2005.09.019.
[14] S. Ivorra, M.J. Palomo, G. Verdú, A. Zasso, Dynamic forces produced by swinging bells, Meccanica. 41 (2006). doi:10.1007/s11012-005-7973-y.
[15] S. Brown, J.-P. Hwang, A. Parker, Assessment of masonry bell tower response to bell ringing using operational modal analysis and numerical modelling, in: Aust. Acoust. Soc. Conf. 2012, Acoust. 2012 Acoust. Dev. Environ., 2012: pp. 25–31.
[16] M. Lepidi, V. Gattulli, D. Foti, Swinging-bell resonances and their cancellation identified by dynamical testing in a modern bell tower, Eng. Struct. 31 (2009) 1486–1500. doi:10.1016/j.engstruct.2009.02.014.
[17] S. Bennati, L. Nardini, W. Salvatore, Dynamic Behavior of a Medieval Masonry Bell Tower. Part I: Experimental Measurements and Modeling of Bell's Dynamic Actions, J. Struct. Eng. 131 (2005) 1647–1655. doi:10.1061/(ASCE)0733-9445(2005)131:11(1647).
[18] S. Bennati, L. Nardini, W. Salvatore, Dynamic Behavior of a Medieval Masonry Bell Tower. Part II: Measurement and Modeling of the Tower Motion, J. Struct. Eng. 131 (2005) 1647–1655. doi:10.1061/(ASCE)0733-9445(2005)131:11(1647).
[19] P. Brzeski, A.S.E. Chong, M. Wiercigroch, P. Perlikowski, Impact adding bifurcation in an autonomous hybrid dynamical model of church bell, Mech. Syst. Signal Process. 104 (2018) 716–724. doi:10.1016/j.ymssp.2017.11.025.
[20] P. Brzeski, T. Kapitaniak, P. Perlikowski, Analysis of transitions between different ringing schemes of the church bell, Int. J. Impact Eng. 85 (2015) 55–66.
[21] P. Brzeski, T. Kapitaniak, P. Perlikowski, Experimental verification of a hybrid dynamical model of the church bell, Int. J. Impact Eng. 80 (2015) 177–184.
[22] J. Heyman, B.D. Threlfall, Inertia forces due to bell-ringing, Int. J. Mech. Sci. 18 (1976).
[23] J. Majer, G. Niederwanger, Observations during stabilization of old bell towers damaged by cracks, Eng. Fract. Mech. 35 (1990) 493–499.
[24] H.P. Wölfel, M. Schalk, Vibration of bell towers [Schwingungen von Glockentürmen], Bautechnik. 73 (1996) 335–347.
[25] S. Bennati, L. Nardini, W. Salvatore, Dynamic Behavior of a Medieval Masonry Bell Tower. Part I: Experimental Measurements and Modeling of Bell's Dynamic Actions, J. Struct. Eng.

131 (2005) 1647–1655.
[26] F.P. Müller, Dynamische und statische Gesichtspunkte beim Bau von Glockentürmen, in: Glocken Geschichte Und Gegenwart, Badenia Verlag GmbH, Karlruhe, 1986: pp. 201–212.
[27] J. Steiner, Neukonstruktion und Sanierung von Glockentürmen nach statischen und dynamischen Gesichtspunkten, in: Glocken Geschichte Und Gegenwart, Badenia Verlag GmbH, Karlruhe, 1986: pp. 213–237.
[28] K.G. Schütz, Dynamische Beanspruchung von Glockentürmen, Bauingenieur. 69 (1994) 211–217.
[29] DIN 4178:1978-08 Glockentürme; Berechnung und Ausführung, (1978).
[30] DIN 4178 2005-04: Glockentürme [In German], (2005) 32.
[31] J.M. Wilson, A.R. Selby, Durham Cathedral tower vibrations during bell-ringing, in: Eng. a Cathedr., n.d.: pp. 77–100. doi:10.1680/eac.16842.0006.
[32] A.R. Selby, J.M. Wilson, Dynamic behaviour of masonry church bell towers, in: Struct. Congr. - Proc., 1996: pp. 188–199.
[33] S. Ivorra, F.J. Pallarés, J.M. Adam, Masonry bell towers: Dynamic considerations, Proc. Inst. Civ. Eng. Struct. Build. 164 (2011).
[34] A. Pau, F. Vestroni, Vibration assessment and structural monitoring of the Basilica of Maxentius in Rome, Mech. Syst. Signal Process. 41 (2013) 454–466.
[35] S. Ivorra, D. Foti, D. Bru, F.J. Baeza, Dynamic behavior of a pedestrian bridge in Alicante, Spain, J. Perform. Constr. Facil. 29 (2015). doi:10.1061/(ASCE)CF.1943-5509.0000556.
[36] M. Betti, L. Facchini, P. Biagini, Damage detection on a three-storey steel frame using artificial neural networks and genetic algorithms, Meccanica. 50 (2015) 875–886. doi:10.1007/s11012-014-0085-9.
[37] NTC2008, Norme tecniche per le costruzioni, D.M. 14/01/2008, Gazz. Uff. 29 (2008) [In Italian].
[38] S. Ivorra, F.J. Pallarés, J.M. Adam, Dynamic behaviour of a modern bell tower - A case study, Eng. Struct. 31 (2009). doi:10.1016/j.engstruct.2009.01.002.
[39] ARTeMIS: Ambient Response Testing and Modal Identification Software, (2016).
[40] P. Bonato, R. Ceravolo, A. De Stefano, F. Molinari, Cross-time frequency techniques for the identification of masonry buildings, Mech. Syst. Signal Process. 14 (2000) 91–109.
[41] C. Chisari, C. Bedon, C. Amadio, Dynamic and static identification of base-isolated bridges using Genetic Algorithms, Eng. Struct. 102 (2015) 80–92. doi:10.1016/j.engstruct.2015.07.043.
[42] DIN 4150 - Vibrations in buildings - Part 3: Effects on stru ctures, (1986).

[43] A.M. D’Altri, G. Castellazzi, S. de Miranda, A. Tralli, Seismic-induced damage in historical masonry vaults: A case-study in the 2012 Emilia earthquake-stricken area, J. Build. Eng. 13 (2017) 224–243. doi:10.1016/j.jobe.2017.08.005.

[44] D. Foti, S. Ivorra Chorro, M.F. Sabbà, Dynamic investigation of an ancient masonry bell tower with operational modal analysis a non-destructive experimental technique to obtain the dynamic characteristics of a structure, Open Constr. Build. Technol. J. 6 (2012). doi:10.2174/1874836801206010384.

[45] G. Abbiati, R. Ceravolo, C. Surace, Time-dependent estimators for on-line monitoring of full-scale structures under ambient excitation, Mech. Syst. Signal Process. 60 (2015) 166–181.

[46] G. Bartoli, M. Betti, A.M. Marra, S. Monchetti, Semiempirical formulations for estimating the main frequency of slender masonry towers, J. Perform. Constr. Facil. 31 (2017). doi:10.1061/(ASCE)CF.1943-5509.0001017.

[47] F.J. Baeza, S. Ivorra, D. Bru, F.B. Varona, Dynamic evaluation of a historic fountain under blast loading, in: Procedia Eng., 2017. doi:10.1016/j.proeng.2017.09.435.

Table 1. Dynamic properties of the bells in the Fiesole bell tower.

Bell	Geometry coefficient	Weight (kg)	Diameter (mm)	Swing velocity		Swing rotation angle (º)	Dynamic Force (kN)
				rev/min	rad/s		Horizontal
Campanone	0.76	728	1120	29.98	3.14	64	5.012
Linara	0.75	448	970	33.52	3.51	73	3.645
Misericordia	0.75	330	870	33.04	3.46	65	2.289
Cantina	0.75	230	780	34.47	3.61	72	1.838
Fratina	0.80	250	670	36.96	3.87	69	2.006

Table 2. Mechanical and Geometrical Properties of similar masonry towers.

Authors	E	ϒ	H	H_{eff}	a	b	s	f_{1exp}
-	MPa	kN/m³	m	m	m	m	m	Hz
Ivorra and Cervera (2001)	1100	16	37	27	4.7	4.7	1.4	0.73
Casciati and Al-Saleh (2010)	1600	18	39	29	5.9	5.9	1.1	1.05
Ivorra and Pallarés (2006)	2500	18	41	28	5.6	5.6	1.2	1.29
Kohnan et al. (2011)	1960	19	41	34	7.6	7.6	1.1	1.37
Zonta et al. (2004)	1700	18	62	39	7.3	7.3	1.3	0.85
Bennati et al. (2005)	1800	18	34	29	7.0	11	1.1	1.20

E: elastic modulus; ϒ: masonry self-weight; H: tower height; H_{eff}*: tower height without lateral constraint walls; a: tower lateral side; b: tower lateral side; s: wall thickness;* f_{1exp}*: first experimental vibration frequency.*

Table 3. Dynamic interaction between bells and tower. Input and output variables for the parametric analysis.

Output variables	**Input variables**			
	Swing velocity	**Swing angle**	**Position height**	**Swing direction**
	rpm	º	m	-
DAF	from 18 to 45 every 0.01	-	-	-
Velocity and displacement	19.8, 24.53, 26.87, 31.2, 31.54, 34.54, 40.11, 44.15	from 50 to 170 every 10	30.9	East-West
			26.3	East-West & North South

Table 4. Statistical analysis of ambient vibration test and FEM model frequencies. Mean natural frequencies for frequency domain decomposition and stochastic subspace identification techniques.

Mode		FDD		EFDD		CFDD		UPC		PC		CVA		FEM model	MAC
-	plane	Hz	csv	Hz	csv	Hz	csv	Hz	csv	Hz	csv	Hz	csv	Hz	Exp/Num
1	zy (N-S)	0.86	*0.03*	0.87	*1.22*	0.89	*1.75*	0.86	*0.33*	0.87	*0.71*	0.86	*0.30*	0.81	0.982
2	zx (E-W)	0.98	*0.02*	0.97	*2.50*	0.98	*0.66*	0.98	*0.51*	0.98	*0.61*	0.98	*0.59*	0.99	0.997
3	xy	3.53	*1.28*	3.55	*0.11*	3.55	*0.09*	3.55	*0.12*	3.57	*1.20*	3.54	*0.06*	3.68	0.992
4	zy (N-S)	3.94	*0.99*	3.94	*1.21*	3.98	*1.91*	3.96	*0.44*	3.99	*0.41*	3.99	*0.19*	4.03	0.738
5	zx (E-W)	4.47	*0.50*	4.48	*0.53*	4.47	*0.51*	4.45	*0.76*	4.46	*0.85*	4.46	*0.76*	4.68	0.928

#: 1-2. 1st bending mode; 3. torsional mode, 4-5; 2nd bending mode.
FDD: Frequency Domain Decomposition; EFDD: Enhanced Frequency Domain Decomposition; CFDD: Curve-fit Frequency Domain Decomposition; UPC: Unweighted Principal Component; PC: Principal Component; VA: Canonical Variate Analysis.

Table 5. Initial range and updated parameters for GA optimization process.

Mode	Parameters optimized				
	E_{w1}	E_{w2}	E_{w3}	E_{t1}	ρ_{t1}
	MPa	MPa	MPa	MPa	Kg/m³
Initial range values	1.2E3-1.2E5	1.2E3-1.2E5	1.2E3-1.2E5	1.1E3-2.5E3	1.6E3-1.9E3
Updated model	1.1678E5 (56%)	6.751E4 (21%)	1.195E5 (67%)	2.04E3 (8.3%)	1.8945E3 (0.2%)

(E_{w1}, E_{w2}, E_{w3}): Equivalent elastic modulus of confinement lateral walls (see Fig. 2).
(E_{t1}, ρ_{t1}): Elastic modulus and self-weight of tower masonry walls.

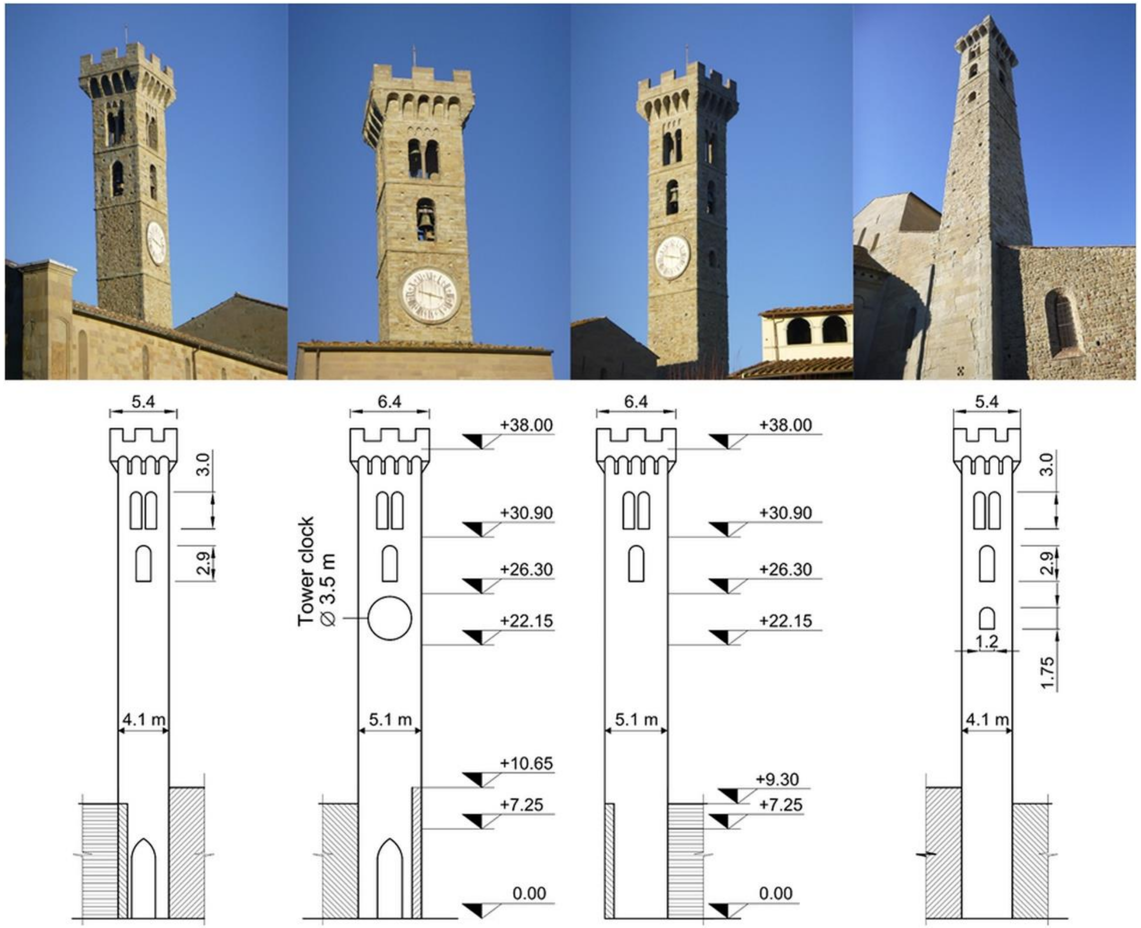

Fig. 1. General and frontal views of Fiesole bell-tower. From left to right: West, South, East and North Faces

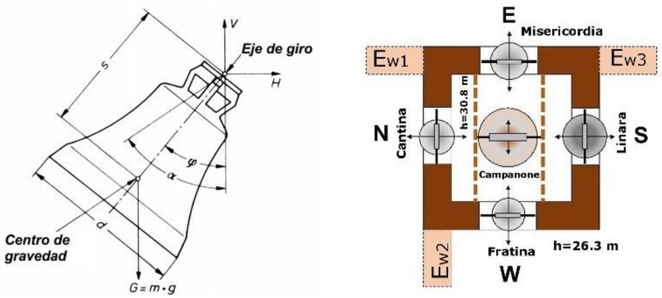

Fig. 2. Left: Simplified bell model. Right: Arrangement of the bells with their swing directions.

Fig. 3. Bells in the Fiesole bell tower. From left to right: a) Campanone. b) Linara. c) Misercordia. d) Cantina. e) Fratina.

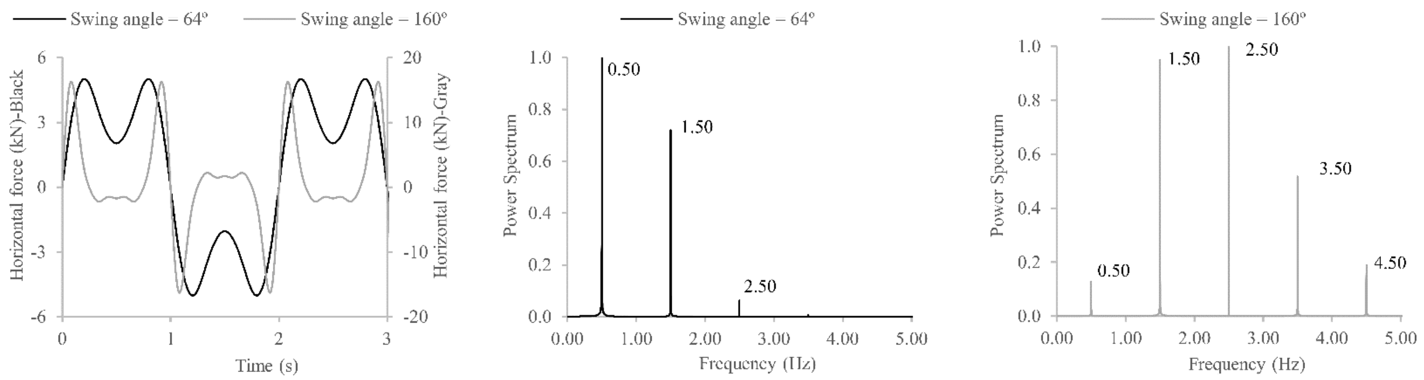

Fig. 4. Example of Campanone's dynamic loads. Left: dynamic loads; Centre: FFT for swing angle of 64º; Right: FFT for swing angle of 160º.

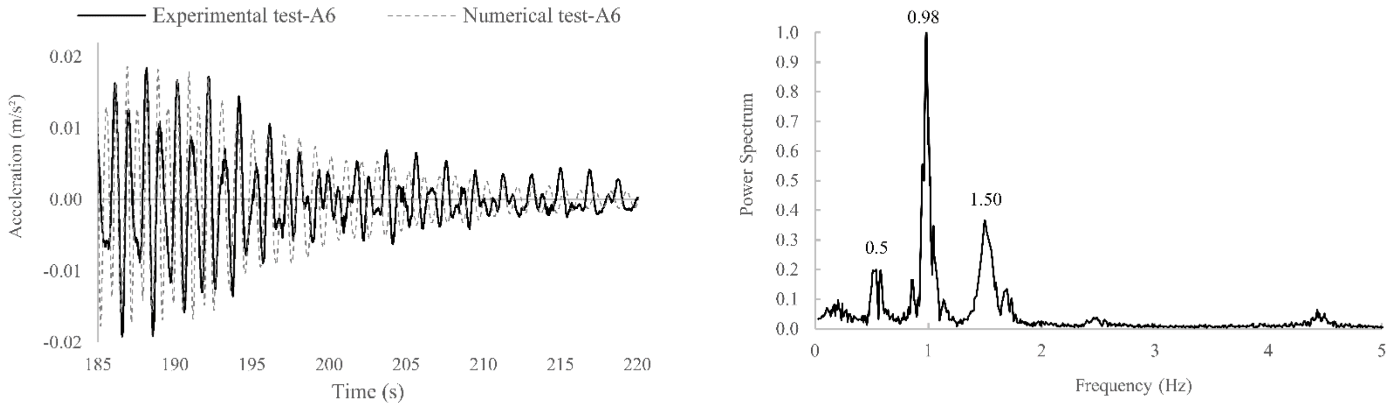

Fig. 5. Misericordia swing test results. Left: Experimental and numerical horizontal accelerations; Right: Experimental FFT analysis for A6.

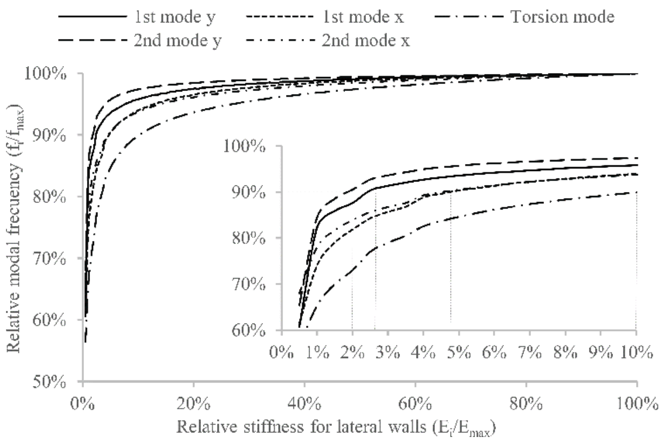

Fig. 6. Modal frequency variation with wall lateral stiffness.

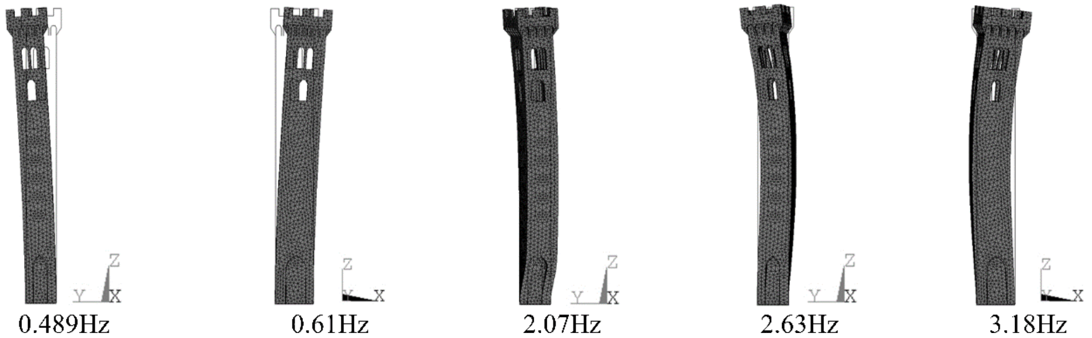

Fig. 7. Modal shapes without lateral walls (Ei/Emax=0%)

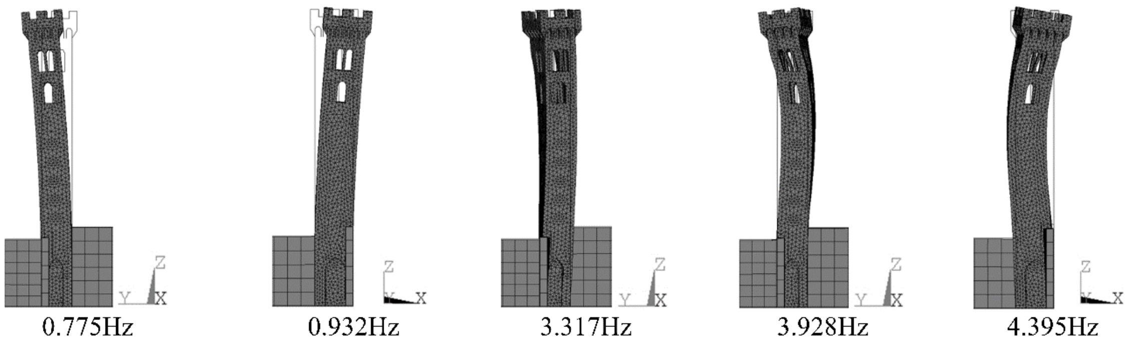

Fig. 8. Modal shapes with lateral walls (Ei/Emax=10%)

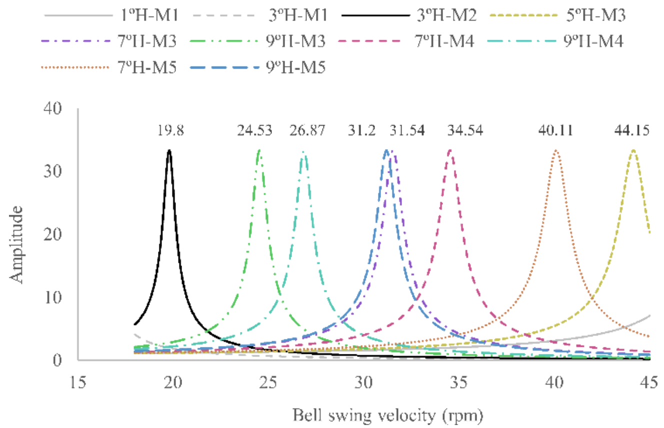

Fig. 9. Local sensitivity analysis of the dynamic interaction between bell tower frequencies and bell harmonics for confined tower.

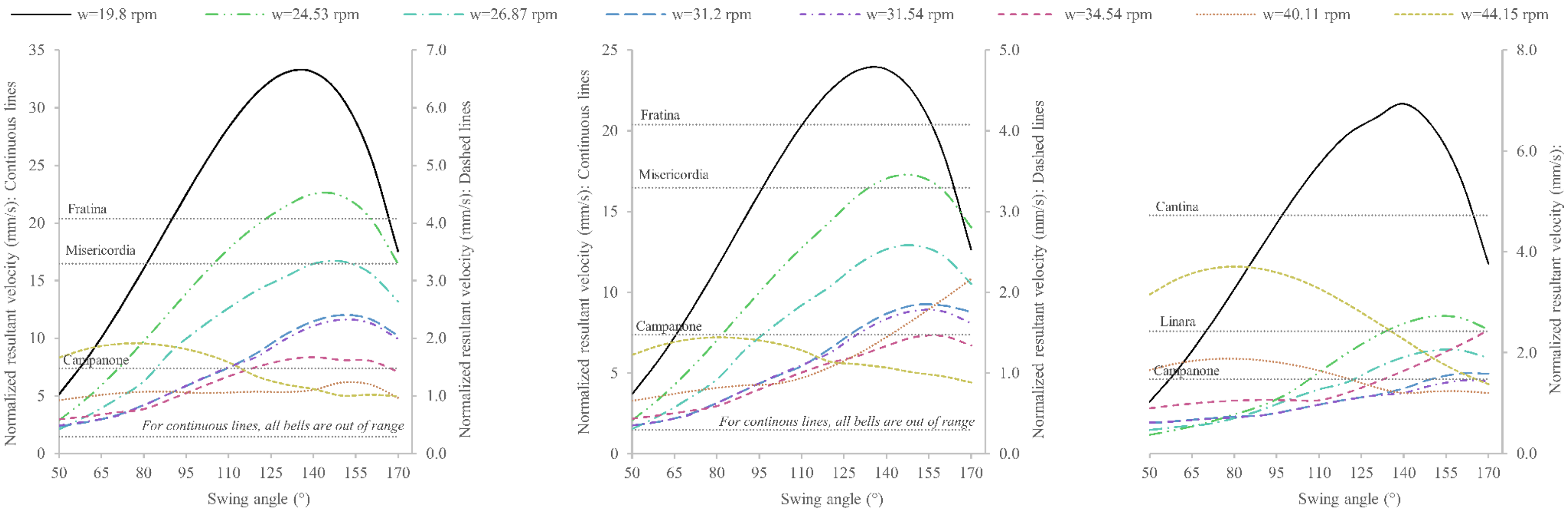

Fig. 10. Maximum horizontal velocity on the last floor (confined tower) for bell loads: Left: 30.9m, E-W; Centre: 26.3m, E-W; Right: 26.3m, N-S.

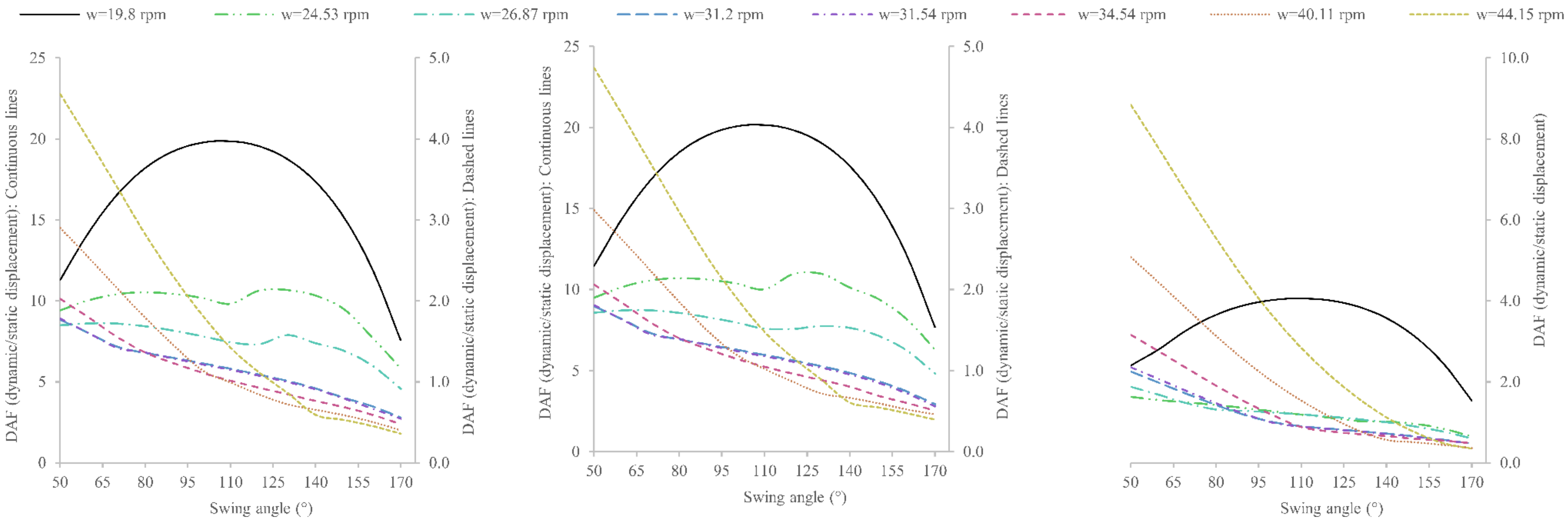

Fig. 11.Relationship between dynamic and static displacements for bell loads. Left: 30.9m, E-W; Centre: 26.3m, E-W; Right: 26.3m, N-S.

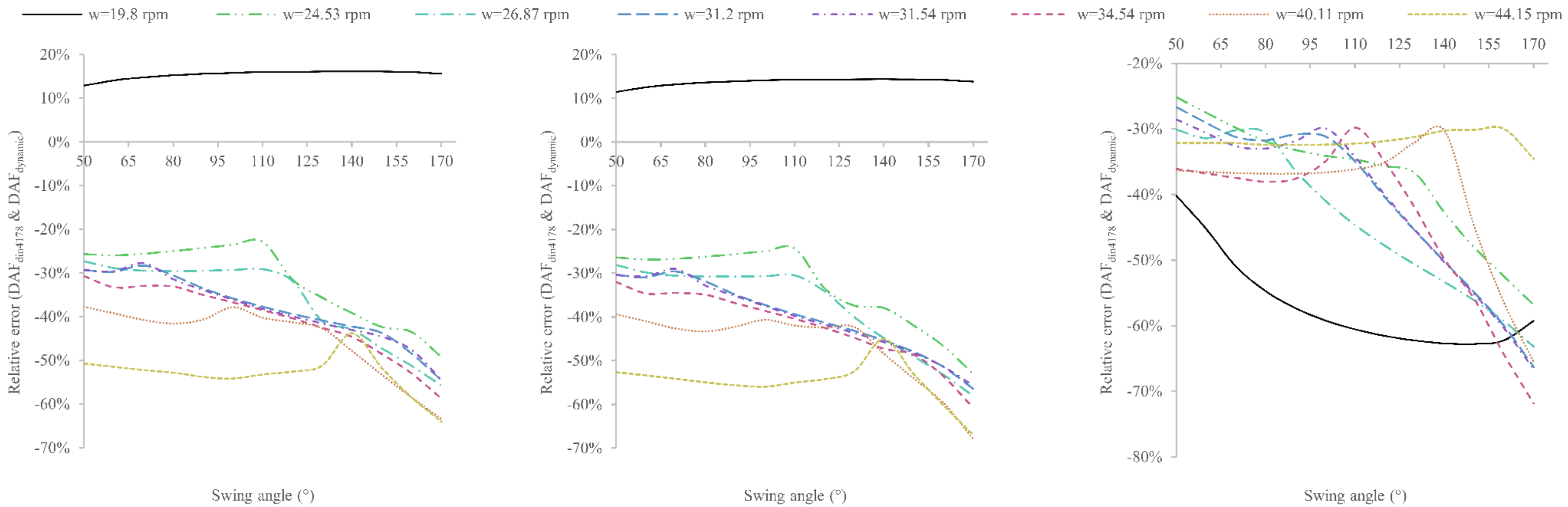

Fig. 12. Relative error of horizontal displacement between DAF$_{din4178-1978}$ & DAF$_{dynamic}$. Left: 30.9m, E-W; Centre: 26.3m, E-W; Right: 26.3m, N-S.

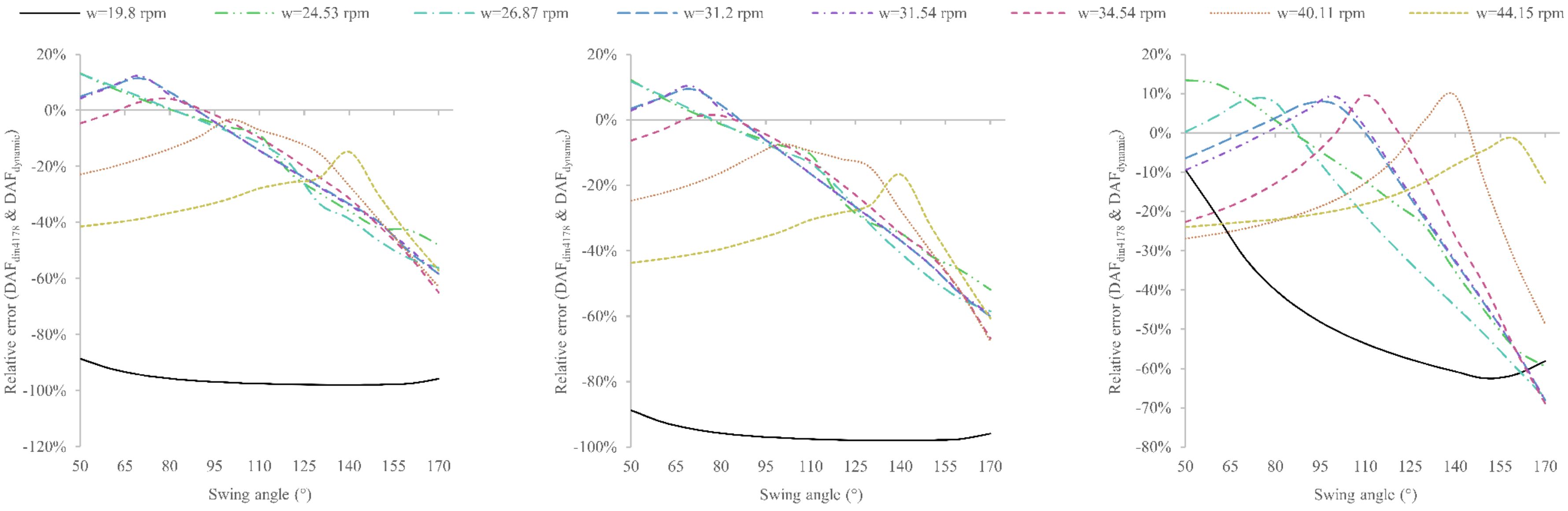

Fig. 13. Relative error of horizontal displacement between $DAF_{din4178-2005}$ & $DAF_{dynamic}$,. Left: 30.9m, E-W; Centre: 26.3m, E-W; Right: 26.3m, N-S.